

Design of High Contrast OPA System for the Vulcan Laser System

Contact: pedro.oliveira@stfc.ac.uk

T. Murphy, P. Oliveira, W. A. Carter, I. O. Musgrave

Central laser facility,
STFC Rutherford Appleton Laboratory
Harwell Campus
OXON. OX11 0QX, UK

Abstract

Temporal contrast is a key feature of any high intensity laser. One method of improving contrast is short pulse Optical Parametric Amplification (OPA). Here we present a new high contrast Optical Parametric Chirped Pulsed Amplifier (OPCPA) for the Vulcan laser system, which is specifically designed for the unique Optical Parametric Oscillator (OPO) system at Vulcan. We start with a review of the current high contrast OPCPA system at the Vulcan laser facility. We discuss the new architecture of picosecond pump laser and present simulations of two different regenerative amplifiers, each with different crystals used as the gain material in the Regenerative Amplifier (RGA), Nd:YLF and Yb:SSO. This is followed by simulations on the nonlinear processes of second harmonic generation (SHG), OPA and the output pulse. An investigation of the relationship of the pump-seed pulse duration and the overall efficiency of the system is carried out. This ratio is then determined in order to maximise the output efficiency of the system. Finally, a scan of the input and output intensities of the pulse is carried out for the OPA, which allowed us to determine the input spectrum and intensity of the pulse for the most stable configuration of the system.

Introduction

Vulcan is a Petawatt laser facility [1, 2] with the ability to deliver pulses with intensities as high as 10^{21} W/cm², and is used for a variety of experiments, ranging from laser astrophysics to plasma physics. These high intensities are achieved using both classical chirped pulse amplification (CPA) and Optical Parametric Chirped Pulse Amplification (OPCPA), which occur in the Front End (FE) of Vulcan [3]. Here, a pump pulse, with energy in the nanojoule level, first travels through a regenerative amplifier (RGA), where it is amplified up [3]. A second harmonic (SH) is then generated, where the frequency of the pump is doubled. Finally, the pump is combined with a seed pulse in an OPA crystal, where the seed pulse

is amplified. [3].

Temporal contrast, is the ratio of the background noise and the main peak pulse [4]. It is one of the most important parameters on any high intensity laser as it may effect any laser plasma interactions carried out[5]. Currently, we have two CPA laser systems in the Vulcan laser facility [1, 2], one with a contrast ratio of 10^8 [6] and a high intensity one with a contrast ratio of 10^{10} . This laser architecture should allow a contrast ratio of 10^{12} beyond a few picoseconds [2].

The overall contrast of the pulse is heavily dependant on the laser architecture of the system. There have been several techniques developed to increase this contrast, amongst them include the use of a nonlinear interferometer [7, 8], cross polarization wave generation [9], saturable absorbers [10] and plasma mirrors [5].

In Vulcan, a femtosecond/picosecond OPA is used to increase the overall contrast, where a pump and seed pulse are superimposed on a nonlinear crystal. As the gain depends exponentially on the pump intensity, this is an instantaneous process. Super-parametric fluorescence is another phenomena that also depends on the gain experienced by the laser [11]. Hence, the overall gain and fluorescence of the system depends heavily on the intensity and spectrum of the pump.

In this contribution, we start with the current system architecture, we then put forward our proposed system architecture we then discuss gain narrowing for two different regenerative amplifiers gain materials that serve as OPA pumps. We present frequency space based nonlinear simulations and scans through crystal lengths, ratio of pulse durations between pump and seed and finally scan of pump intensity for maximum stability.

Current OPCPA system architecture at Vulcan

A schematic of the current OPCPA in Vulcan can be seen in Fig 1.

The 80MHz, nanojoule, hard aperture mode locked Ti:sapphire laser oscillator is split in two, of which 90% of this laser goes to a Nd:YLF RGA that amplifies it to the millijoule level. The RGA currently in use at Vulcan is a flash lamp pumped Nd:YLF laser. In this system, the laser is stretched to 10 ps at 1 mJ, due to phenomena such as dispersion and gain narrowing. This pulse is then

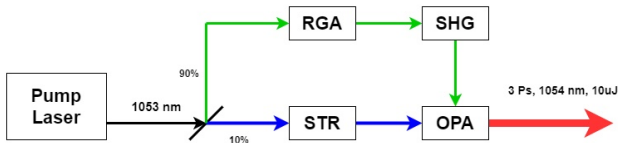


Figure 1: Current Architecture at Vulcan FE

frequency doubled, through the process of SHG, to 527 nm with energy 0.5 mJ. It is this 0.5 mJ laser SH laser that is used as a pump for the OPCPA.

The remainder of the pulse is stretched on a zero delay line to 3 ps and superimposed with the pump on an OPA crystal. The effective gain experienced by the pulse is approximately 10^4 , however the actual gain on the crystals due to OPA is 2×10^5 . The OPA is done in a BBO Type-I crystal, 15 mm in length and width. The OPCPA process is close to degeneracy, which requires us to place a small non-collinear angle between the pump and seed. This will allow us to distinguish between the seed and the idler as they exit the OPA. A laser beam of 10 μ J at 1054 nm with pulse duration 3 ps is produced, which then exits the OPCPA system.

Future OPCPA system architecture at Vulcan

We present two possible future system architecture for the OPCPA system at Vulcan, one which uses the customary, well established RGA crystal (Nd:YLF) and another which uses an unconventional crystal (Yb:SSO) with the potential to achieve high contrast in the OPCPA system. The general schematic is given in Figure 2.

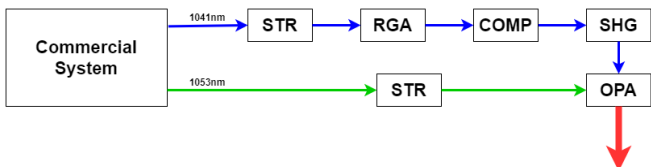


Figure 2: Proposed Architecture at Vulcan FE

One of the oscillators currently in use at Vulcan is an Optical Parametric Oscillator (OPO) system, this is the commercial system in Figure 2. This OPO has part of it's pump exiting the system at 1041 nm as well as a second laser output, which is tunable from 680 - 1300 nm. At 1053 nm the beam has a Gaussian profile with a bandwidth of 15 nm, 80 MHz, 1 W. Both outputs are intrinsically optically synchronized. In our proposed architecture the 1041 nm pulse will be amplified in a CPA system with an RGA. This undergoes SHG. It is then superimposed with the 1053 nm seed pulse in an OPA, amplifying the seed pulse and exits the OPCPA. Throughout this report, we simulate the proposed architecture and determine the parameters of the system

required to maximise conversion efficiency of each stage. We then simulate the output pulse of the OPA and determining the relationship between pulse duration and conversion efficiency.

Regenerative Amplifier

Theory

Temporal Contrast

The pump laser is initially amplified using a RGA, which is commonly used to amplify pulses from nanojoules to millijoules. To do so, a gain medium and optical switch are placed inside an optical resonator. As a pulse of light passes through the resonator, it gets trapped by the optical switch. It is amplified through the gain medium which can be described by the following Eq. 1

$$G = e^{(\sigma N_2 z)} \quad (1)$$

where G is the gain, σ is the emission spectrum and is dependant on wavelength, and z is the length of the crystal in the RGA. The output spectrum of the pulse can then be described by the following equation:

$$S_1(\lambda) = S_0(\lambda)e^{(\sigma(\lambda)N_2 z)} \quad (2)$$

Note that the above equation is only relevant for a single pass in the RGA. For a multi pass RGA, where the pulse passes through the gain medium many times, the spectrum after the i^{th} pass can be described by:

$$S_i(\lambda) = S_{i-1}(\lambda)e^{(\sigma(\lambda)(N_2(i)+N_2(i-1)+\dots+N_2(1))z)} \quad (3)$$

where $N_2(i)$ is the population inversion inside the gain medium after the i^{th} pass. The number of round trips can be controlled by the switch, and can be very large, leading to a high gain. After a sufficient amount of gain, the pulse of light leaves the resonator and is used as the pump for the OPCPA system.

Numerical Simulation

When simulating the multipass RGA used at Vulcan, we approximate the multipass RGA as a single pass RGA with a gain described by:

$$G = e^{(\sigma(\lambda)\gamma)} \quad (4)$$

where,

$$\gamma = (N_2(i) + N_2(i-1) + \dots + N_2(1))z \quad (5)$$

To determine γ we assume the initial 1053 nm pump pulse with energy 8.75 nJ is amplified to 20 mJ. Using equation 4 we can then determine γ , which is then used to determine the overall output spectrum of the RGA for different crystals, each with different gain bandwidths.

Please note, the overall loss of the system will also affect the overall gain narrowing of the laser pulse as it passes through the RGA. This is mainly due to the increase in the number of passes in order to achieve a similar gain when compared to a system with no loss. To include losses in the RGA, we assume a single pass has a loss of 10%. We also assume the laser passes through the RGA 100 times, with a coupling efficiency of 90%. Using these values, one can approximate the overall loss of the RGA to be approximately 10^{-6} . This value was then used as the overall loss of the system.

Results and Discussion

The initial seed of the RGA pulse used throughout the simulation can be seen in Figure 3.

This pulse was used as the input spectrum when simulating a multipass RGA, using the approximations as described above in the Numerical Simulations section. Two different multipass amplifiers were simulated, each containing different gain material, Nd:YLF and Yb:SSO. These two crystals have different emission cross sections, as seen below in Figure 3.

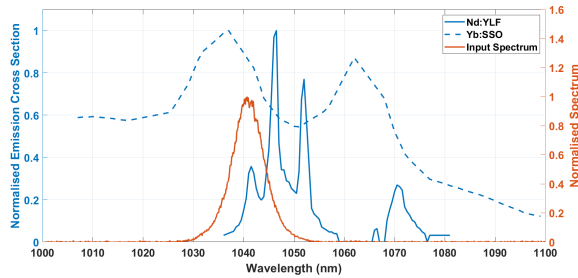


Figure 3: Normalised Emission Cross Sections of Nd:YLF and Yb:SSO and the Normalised Input Spectrum for the RGA

Hence, according to Equation 4, this will lead to different gain spectrums, and hence different output pulses for each RGA. The two output spectrums were simulated and can be seen in Figures 4 and 5. The characteristics of the output pulse can be seen below in Table 1

Output Characteristics of RGA		
Crystal Type	Nd:YLF	Yb:SSO
FWHM (ps)	2.2	0.2
Intensity($W\ cm^{-2}$)	10^{10}	10^{10}
Energy (mJ)	20	20
Bandwidth (PHz)	7.5×10^{-4}	3.6×10^{-3}
Central Wavelength (nm)	1047	1037

Table 1: Characteristics of Output Pulses of RGA

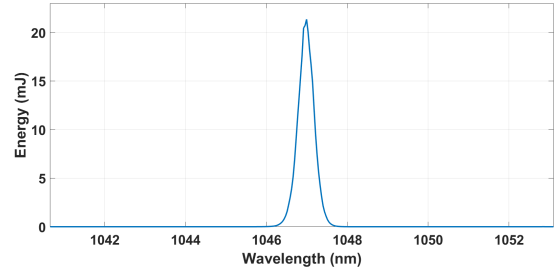


Figure 4: Output pulse of Nd:YLF RGA

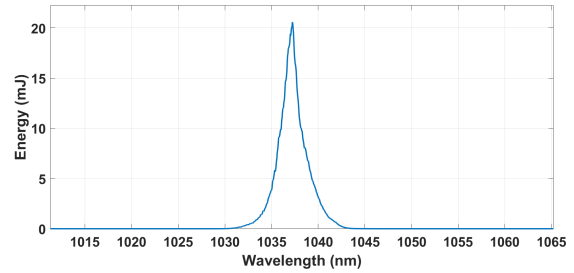


Figure 5: Output pulse of Yb:SSO RGA

The characteristics of the output pulses of both RGA can be seen in Table 1. These output pulses were then used as the initial pulse for the next stage of our OPCPA, SHG.

We had simulated other Nd and Yb doped materials. However, they did not have emission peaks within the OPO pump, and no further investigations with these materials were carried out. Another reason to consider Yb:SSO instead of Nd:YLF is that it is pumped at 980 nm instead of 808 nm and that its fluorescence time is substantially higher, the two things combined mean that the pump diodes can be up to 6 times less powerful which might decrease the cost of any RGA.

OPA

Theory

Nonlinear Optical Phenomena (Second Harmonic Generation and Difference Frequency Generation)

Nonlinear optical processes occur when a pulse of light and material interact with each other in a nonlinear manner. Typically, the ability for a material to behave in a nonlinear manner is represented by the material's nonlinear susceptibility, χ . Typical values of χ are found to be of the order of 10^{-12} V/m for both BBO and LBO.

As a result of these nonlinear interactions, new pulses are produced as a laser passes through a crystal with high nonlinear susceptibility. Two examples of this are second harmonic (SH) and Difference Frequency Generation (DFG). SHG occurs when a pulse of light travels

through a nonlinear crystal and interacts with itself, creating a new pulse with double the frequency, called its SH. This nonlinear process is used to double the frequency of the laser in the OPA system. DFG is when two different pulses of light, a 'pump' and 'seed', travel through a nonlinear crystal simultaneously, where the pump's energy is initially much higher than the energy of the seed. This creates a new pulse, whose frequency spectrum is the difference between the two initial pulses. This new pulse is commonly called the idler. As the idler is produced the seed pulse is amplified while the pump pulse is depleted.

Numerical Simulation

Second Harmonic Generation (SHG) and Optical Parametric Amplification (OPA) Simulations

The simulations completed in this report were carried out in the frequency domain. This enhances the importance of the different group delays, amongst the several frequencies of the beam. This method is also the most appropriate way of simulating pulses close to transform limit. We take the three wave mixing equation from [12] both SHG and OPA can be described by the following coupled differential equations:

$$\frac{dA_0(\Omega)}{dz} = \frac{i\omega_0}{2cn}\chi \int A_1(\omega_1)A_2(\Omega - \omega_1)e^{i\Delta kz} d\omega \quad (6)$$

$$\frac{dA_1(\Omega)}{dz} = \frac{i\omega_1}{2cn}\chi \int A_0(\omega_0)A_2^*(\Omega - \omega_0)e^{-i\Delta kz} d\omega \quad (7)$$

$$\frac{dA_2(\Omega)}{dz} = \frac{i\omega_2}{2cn}\chi \int A_0(\omega_0)A_1^*(\Omega - \omega_0)e^{-i\Delta kz} d\omega \quad (8)$$

where A is the amplitude of the electric field, ω and Ω represent the frequency of the pulse, z is the length of the crystal, Δk is the phase mismatch, χ is the nonlinear coefficient of the crystal, c is the speed of light and n is the index of refraction. Throughout the simulations in this report, the nonlinear crystal was used with $\chi = 4.2 \times 10^{-12} \text{Vm}^{-1}$

For Second Harmonic (SH) Generation we note that

$$\omega_0 = 2\omega_1 \quad (9)$$

and $\omega_1 = \omega_2$, where A_0 is the generated pulse. A_1 and A_2 are the initial pump from the RGA. From these equations, one can see that as the pump travels through the nonlinear crystal, it decreases in amplitude, while the SH is generated. Because the pulses aren't single linewidth there is a sweep of sum of frequencies that result on the same frequency on the second harmonic. In order to solve this, we had to iterate both spectrums with the same spacing between points and that the value of frequency in the array is an integral number of the spacing.

For Difference Frequency Generation we note that

$$\omega_0 = \omega_1 + \omega_2 \quad (10)$$

Here we note that A_0 is the SH pulse generated in the previous step of the OPCPA system, A_1 is the seed, which is to be amplified and A_2 is the idler pulse generated throughout the process. It is evident from the coupled equations that as the pump and seed travel through the crystal, the seed is amplified while the pump is being depleted and a third pulse, the idler is generated.

These equations were first normalised and solved in the frequency domain using both the Runge Kutta Method and the Euler method in order to simulate the propagation of the three pulses throughout the crystal. Throughout this simulation, the pulses were a range of different frequencies and therefore one must take into account the convolution of the two amplitudes in the equations, which determine the growth of each pulse.

Results and Discussion

SHG Simulation

Using the equations 6 to 8 the initial pulses evolution throughout a BBO crystal was simulated and the overall conversion efficiency was calculated throughout its propagation. The conversion efficiencies throughout this simulation can be seen below in Figures 6 and 7. In both cases the peak intensity of the pulse was 10^{10}W/cm^2 .

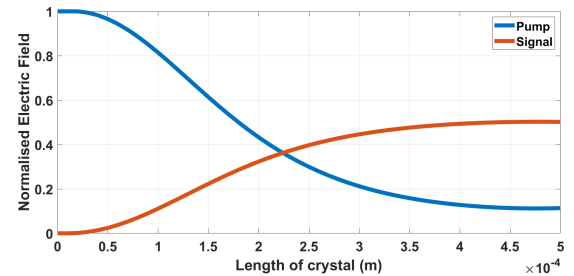


Figure 6: Conversion Efficiency of the SHG with respect to length. Here the input pulse is from the Yb:SSO RGA

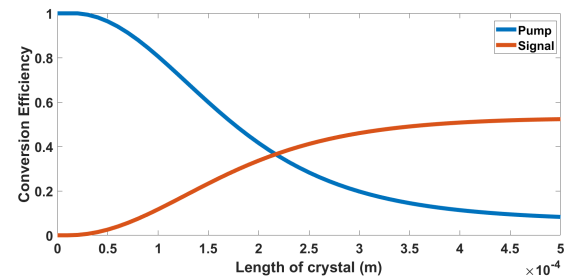


Figure 7: Conversion Efficiency of the SHG with respect to length. Here the input pulse is from the Nd:YLF RGA

The output of the spectrums can be seen in Table 2.

Output Characteristics of SHG		
Crystal Type RGA	Nd:YLF	Yb:SSO
Length of Crystal (mm)	0.5	0.5
Efficiency (%)	0.50	0.53
Pulse Duration (ps)	1.90	0.26
Central Wavelength (nm)	550	519

Table 2: Output characteristics of the OPA pulses

OPA Simulation

The output spectrums of the SHG simulation were then used to simulate the OPA, where the SH amplifies the seed in the process of DFG. The initial seed was set to have a pulse duration of 120 fs, intensity 7×10^4 W/cm² and energy of 8.75 nJ. Using the approximations, as described in the numerical simulation section, the output spectrums are seen below in Figures 9 and 8. The characteristics of the overall output pulse of the OPA can be seen in Table 3. In all cases we kept the peak intensity at 10^{10} W/cm².

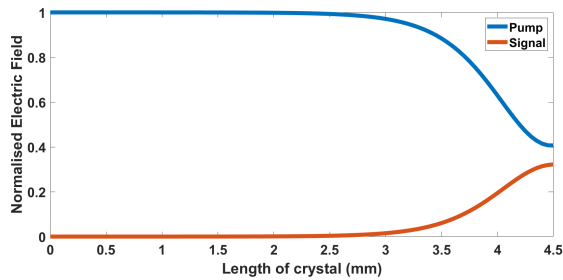


Figure 8: Conversion Efficiency of the OPA with respect to length. The input pulse being the SH of the Yb:SSO RGA

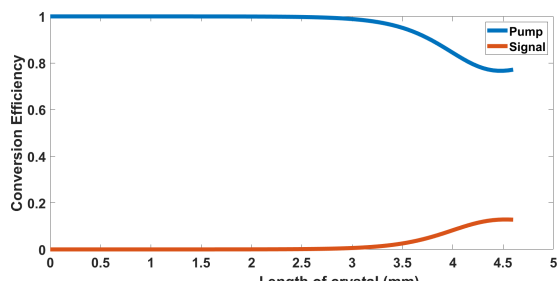


Figure 9: Conversion Efficiency of the OPA with respect to length. The input pulse being the SH of the Nd:YLF RGA

Discussion on Simulation

Comparing the results of both OPCPA simulations, one can see that we can decrease the pulse duration significantly, 0.8 ps and 0.2 ps, when comparing to our current

Output Characteristics of OPA		
Crystal Type RGA	Nd:YLF	Yb:SSO
Length of Crystal (mm)	0.5	0.5
Efficiency (%)	0.13	0.29
Pulse Duration (ps)	0.80	0.31
Central Wavelength (nm)	1054	1052

Table 3: Output Characteristics of the OPA simulation

design of the OPCPA system at Vulcan. This increases the contrast of our overall pulse, which is desirable for the various experiments carried out at Vulcan laser facility. The efficiency of the pulse can be increased by replacing the Nd:YLF RGA, currently used at Vulcan to a multipass RGA containing a different gain material, Yb:SSO. Using this gain material, the efficiency of the OPA can be increased by a factor of 2 from 13% to 29%.

Dependence on pulse duration

After SHG, the seed pulse was then stretched to various lengths before entering the OPA. The maximum efficiency possible and the output seeds bandwidth for each pulse duration was determined by changing the length of the nonlinear crystal. The results can be seen in Figure 10.

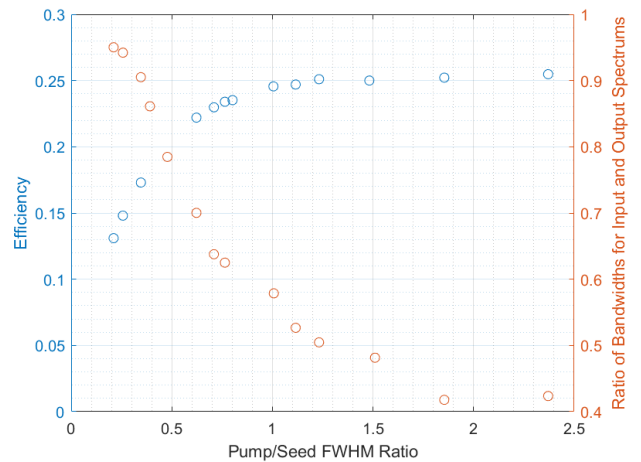


Figure 10: Relationship between Pump/Seed FWHM Ratios, Efficiency and Bandwidth of the output Seed of the OPA

In order to obtain maximum conversion efficiency of the OPA, one must have the pump and seed durations to be approximately equal, as seen from Figure ???. When the durations are equal, the seed can exploit the full spectrum of the seed and obtain the maximum energy possible from the pump. One can also see from Figure ???. When the seed is greater than the pumps, the maximum conversion efficiency then saturates, as the seed has already taking advantage of the energy of the whole pump's spectrum.

Intensity Dependence

A scan of different input intensities was carried out for the OPA. The output intensities were obtained and can be seen in Figure 11.

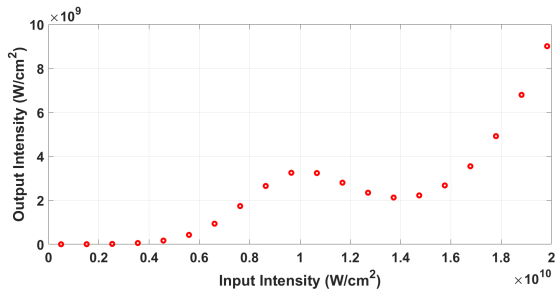


Figure 11: Input Intensity vs Output Intensity of OPA system

In Figure 11, one can see that the local maximum and minimum of this relationship is at 10^{10} W/cm² and 1.4×10^{10} W/cm². At these intensities, the systems output intensity is most stable and the output intensity is not affected by small fluctuations of the input intensity. The output spectrums of both stability points can be seen below in Figure 12.

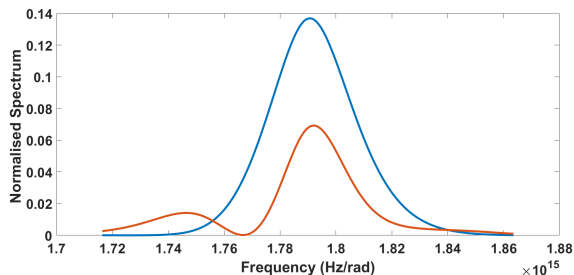


Figure 12: Output Spectrum of OPA. Here the blue spectrum represents the output spectrum of the OPA with input intensity of 10^{10} W/cm² and the orange with input intensity of 1.4×10^{10} W/cm².

Conclusion

To conclude, a study of the architecture of the Vulcan high contrast OPCPA was carried out and both the intensity stability and the gain narrowing effect on the OPCPA has been simulated for the first time in the Fourier domain.

We simulated two possible regenerative amplifiers one using the well known Nd:YLF and an unconventional crystal, Yb:SSO, as the gain material. In the first case simple gain narrowing makes the minimum available pulse duration to be 2.2 ps and the second 200 fs.

We have used these minimum pulse durations to simulate the nonlinear processes in our architecture and retrieve the crystal lengths for the maximum conversion ef-

iciency of each stage of the OPCPA. The SHG efficiency was approximately 50% in both cases. In the first OPA simulation the seed was a 120 fs Fourier limited pulse centered at 1053nm. From these we could observe that the efficiency of the simulation containing the Nd:YLF RGA was 13% and the simulation containing the Yb:SSO RGA was twice as much or 29%. We attributed this to the fact that the pulse duration between the pulses was very different.

We used this system to scan the bandwidths and the pulse duration between the pump and seed pulse at the OPA stage. We can conclude that in order to maximize the efficiency of the OPCPA, the ratio of pulse duration between the seed and the pump before entering the OPA must be approximately one. When this condition is met, the seed can exploit the full energy of the pump. However, based on our results, the pulse spectrum will narrow by almost 40%. Comparing this simulation with the Fourier limited duration of the Yb:SSO, we can see that the efficiency of the process of the chirped pulse never reaches the 29% of the Fourier limited one. At the same ratio of pulse durations as of the the Yb:SSO (a factor of 2) the Nd:YLF efficiency is only 20%. Hence, the process is not only explainable by the pulse durations but also by the existence of the wavelengths phase matching.

Finally, a scan is carried out of the pulse intensity and a plot of the output intensity is obtained. Our objective was to compare the most stable region of the output intensity by comparison with the intensity at maximum conversion. From our simulations, we can conclude that both these intensities were the same.

References

- [1] C. Danson, P. Brummitt, R. Clarke, J. Collier, B. Fell, A. Frackiewicz, S. Hancock, S. Hawkes, C. Hernandez-Gomez, P. Holligan, M. Hutchinson, A. Kidd, W. Lester, I. Musgrave, D. Neely, D. Neville, P. Norreys, D. Pepler, C. Reason, W. Shaikh, T. Winstone, R. Wyatt, and B. Wyborn, “Vulcan petawatt—an ultra-high-intensity interaction facility,” *Nuclear Fusion*, vol. 44, pp. S239–S246, nov 2004.
- [2] C. Hernandez-Gomez, P. Brummitt, D. Canny, R. Clarke, J. Collier, C. Danson, A. Dunne, B. Fell, A. Frackiewicz, S. Hancock, S. Hawkes, R. Heathcote, P. Holligan, M. Hutchinson, A. Kidd, W. Lester, I. Musgrave, D. Neely, D. Neville, and B. Wyborn, “Vulcan petawatt-operation and development,” *Journal de Physique IV (Proceedings)*, vol. 133, 06 2006.
- [3] I. Musgrave, W. Shaikh, M. Galimberti, A. Boyle, C. Hernandez-Gomez, K. Lancaster, and R. Heathcote, “Picosecond optical parametric chirped pulse

- amplifier as a preamplifier to generate high-energy seed pulses for contrast enhancement,” *Appl. Opt.*, vol. 49, pp. 6558–6562, Nov 2010.
- [4] M. P. Kalashnikov and N. Khodakovskiy, “Temporal contrast issues of high peak power Ti:sapphire lasers (Conference Presentation),” in *High-Power, High-Energy, and High-Intensity Laser Technology IV* (J. Hein and T. J. Butcher, eds.), vol. 11033, International Society for Optics and Photonics, SPIE, 2019.
- [5] Y. Arikawa, S. Kojima, A. Morace, S. Sakata, T. Gawa, Y. Taguchi, Y. Abe, Z. Zhang, X. Vaisseau, S. H. Lee, K. Matsuo, S. Tosaki, M. Hata, K. Kawabata, Y. Kawakami, M. Ishida, K. Tsuji, S. Matsuo, N. Morio, T. Kawasaki, S. Tokita, Y. Nakata, T. Jitsuno, N. Miyanaga, J. Kawanaka, H. Nagatomo, A. Yogo, M. Nakai, H. Nishimura, H. Shiraga, S. Fujioka, F. Group, L. Group, H. Azechi, A. Sunahara, T. Johzaki, T. Ozaki, H. Sakagami, A. Sagisaka, K. Ogura, A. S. Pirozhkov, M. Nishikino, K. Kondo, S. Inoue, K. Teramoto, M. Hashida, and S. Sakabe, “Ultra-high-contrast kilojoule-class petawatt laser using a plasmamirror,” *Appl. Opt.*, vol. 55, pp. 6850–6857, Sep 2016.
- [6] M. Galletti, C. Coyle, P. Oliveira, M. Galimberti, F. Bisesto, and D. Giulietti, “VULCAN and FLAME ultra-short pulses characterization by GROG algorithm,” *Journal of Instrumentation*, vol. 14, pp. C02005–C02005, feb 2019.
- [7] E. A. Khazanov and S. Y. Mironov, “Nonlinear interferometer for increasing the contrast ratio of intense laser pulses,” *Quantum Electronics*, vol. 49, pp. 337–343, apr 2019.
- [8] A. Renault, F. Augé-Rochereau, T. Planchon, P. D’Oliveira, T. Auguste, G. Chériaux, and J.-P. Chambaret, “Ase contrast improvement with a nonlinear filtering sagnac interferometer,” *Optics Communications*, vol. 248, no. 4, pp. 535–541, 2005.
- [9] A. Jullien, O. Albert, F. Burgy, G. Hamoniaux, J.-P. Rousseau, J.-P. Chambaret, F. Augé-Rochereau, G. Chériaux, J. Etchepare, N. Minkovski, and S. M. Saltiel, “10¹⁰ temporal contrast for femtosecond ultraintense lasers by cross-polarized wave generation,” *Opt. Lett.*, vol. 30, pp. 920–922, Apr 2005.
- [10] J. H. Sung, S. K. Lee, T. M. Jeong, and C. H. Nam, “Enhancement of temporal contrast of high-power femtosecond laser pulses using two saturable absorbers in the picosecond regime,” *Applied Physics B*, vol. 116, pp. 287–292, Aug 2014.
- [11] V. Bagnoud, J. D. Zuegel, N. Forget, and C. L. Blanc, “High-dynamic-range temporal measurements of short pulses amplified by opcpa,” *Opt. Express*, vol. 15, pp. 5504–5511, Apr 2007.
- [12] R. W. Boyd, *Nonlinear Optics, Third Edition*. USA: Academic Press, Inc., 3rd ed., 2008.